Strathprints Institutional Repository

Parrotta, Daniele C. and Casula, Riccardo and Penttinen, Jussi-Pekka and Leinonen, Tomi and Kemp, Alan J. and Guina, Mircea and Hastie, Jennifer E. (2016) InGaAs-QW VECSEL emitting >1300nm via intracavity Raman conversion. Proceedings of SPIE, 9734. ISSN 0277-786X , http://dx.doi.org/10.1117/12.2217593

This version is available at http://strathprints.strath.ac.uk/57665/

InGaAs-QW VECSEL emitting >1300-nm via intracavity Raman conversion

Daniele C. Parrotta[a*], Riccardo Casula[a], Jussi-Pekka Penttinen[b], Tomi Leinonen[b], Alan J. Kemp[a], Mircea Guina[b], and Jennifer E. Hastie[a]

[a]Institute of Photonics, Department of Physics, University of Strathclyde, Technology and Innovation Centre, 99 George Street, Glasgow G1 1RD, UK
[b]Optoelectronics Research Centre, Tampere University of Technology, Korkeakoulunkatu 3, FIN-33101 Tampere, Finland

ABSTRACT

We report intracavity Raman conversion of a long-wavelength InGaAs-QW VECSEL to ~1320 nm, the longest wavelength yet achieved by a VECSEL-pumped Raman laser. The setup consisted of a VECSEL capable of emitting >17 W at 1180 nm and tunable from 1141-1203 nm and a 30-mm-long KGd(WO₄)₂ (KGW) Raman crystal in a coupled-cavity Raman resonator. The Raman cavity was separated from the VECSEL resonator by a tilted dichroic mirror, which steers the Raman beam to an output coupler external to the VECSEL. The spectral emission of the VECSEL, and consequently of the Raman laser, was set by a 4-mm-thick quartz birefringent filter in the VECSEL cavity. The KGW Raman laser was capable of emitting 2.5 W at 1315 nm, with M^2~2.7 and >4% diode-to-Stokes conversion efficiency. The Raman laser emission was tunable from 1295-1340 nm, limited by the free spectral range of the birefringent filter. Spectral broadening of the fundamental emission was observed during Raman conversion. At the maximum Raman laser output power, the total linewidth of the VECSEL spectrum was ~0.7 nm FWHM. As a consequence, the Raman laser emission was also relatively broad (~0.9 nm FWHM). Narrow (<0.2 nm FWHM) Raman emission was obtained by inserting an additional 100 μm etalon within the VECSEL cavity. With this configuration the fundamental intracavity power clamped at its value at the Raman threshold, suggesting an enhanced effective Raman gain, but the maximum output power of the Raman laser was 1.8 W.

Keywords: Optically pumped semiconductor laser, Raman laser, tuning, VECSEL

1. INTRODUCTION

Vertical-external-cavity surface-emitting lasers (VECSELs) can emit several Watts in continuous-wave (CW) operation with good beam quality and low noise. With the insertion of an intracavity birefringent filter (BRF), VECSELs can also exhibit broad tunability (>300 cm⁻¹ [1]). VECSELs can emit over a broad range of wavelengths via bandgap engineering [1, 2]; however there are certain spectral regions that cannot be easily accessed directly by VECSELs. The most mature VECSEL technology is based on InGaAs quantum wells (QWs), which are capable of efficient laser emission from ~920-1180 nm [3–5]. Due to their high intracavity fields, InGaAs-based structures are well-suited for intracavity nonlinear conversion, thus allowing laser operation in the visible via second harmonic generation [1, 2] and the mid-infrared via optical parametric oscillation [6].

To date, VECSEL operation at ~1300-1400 nm has been obtained either by adding nitrogen in the InGaAs lattice (e.g. GaInNAs QWs [7]) or using wafer-fused InAlGaAs/InP-based gain structures [8]. While dilute nitride structures are capable of emitting several Watts at ~1200 nm [9], their performance drops significantly at longer wavelengths. On the other hand InP-based wafer-fused structures are capable of multi-Watt emission with high conversion efficiency (>50% in [10]), but their fabrication process is quite complex.

Here we propose Raman conversion of a long-wavelength (~1180 nm) InGaAs VECSEL as an alternative way to achieve laser operation at >1300 nm. Intracavity-pumped Raman lasers are a convenient means to red-shift

---

* daniele.parrotta@strath.ac.uk

the emission wavelength of several continuous wave lasers [11,12], including VECSELs [13–15]. The Stokes shift induced by stimulated Raman scattering is a fixed property of the Raman medium, and, unlike second-order nonlinearities, is an intrinsically phase-matched process. With the use of an intracavity wavelength filter (e.g. birefringent filter, etalon), the broad tunability of the VECSEL can be directly transferred to the Stokes shifted output.

2. VECSEL GAIN STRUCTURE AND CHARACTERIZATION

2.1 Gain chip design

The design of the 1180 nm VECSEL is similar to the one reported in [5,16] and is illustrated in Figure 1. The gain chip semiconductor layer structure had 10 InGaAs/GaAs QWs with a nominal indium mole fraction of 37%. The 7 nm-thick quantum wells were located inside the active region at the anti-nodes of the optical standing wave. Relaxation of the highly-strained quantum wells was avoided by growing the QWs at a low growth temperature of 460 °C. Also, strain compensation layers, made of GaAsP a with phosphorus mole fraction of 11%, were located between QWs and between the first QW and the DBR. The DBR had 25.5 pairs of alternating AlAs/GaAs layers. The gain chip was designed anti-resonant at the signal wavelength. On top of the active region, a 20 nm AlGaAs window layer and 10 nm GaAs capping layer were grown.
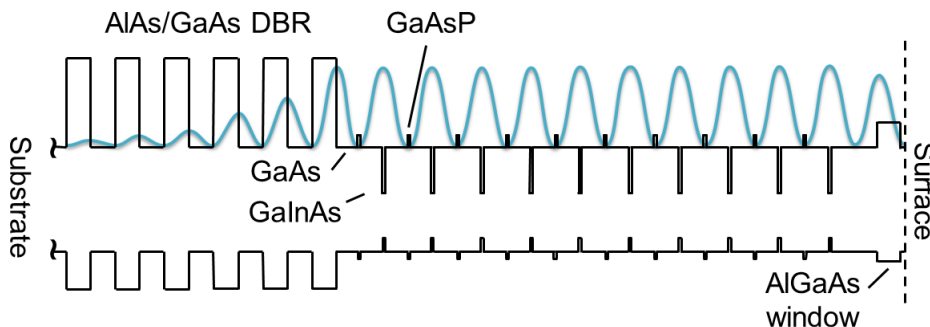

Figure 1. Schematic illustration of the VECSEL gain structure.

2.2 Laser characterization

The 1180 nm VECSEL chip was first tested in a 3-mirror cavity with a curved highly reflective (HR) folding mirror (R>99.98% at 1160-1200 nm, ROC = 200 mm) and a flat output coupler (OC) as the end mirror (see Figure 2). The pump laser was a commercial 808 nm diode laser and its output beam was focused up to a ∼240 µm radius spot on the gain chip with an angle of incidence of ∼40°. For thermal management, the gain chip was capillary-bonded to a wedged (∼2°) 300 µm-thick single-crystal diamond heatspreader. An antireflection coating designed for 1180 nm was deposited on the outer surface of the intracavity heatspreader. The distances between the elements were chosen to be: VECSEL-HR = 110 mm and HR-OC = 170 mm. With 1.6% output
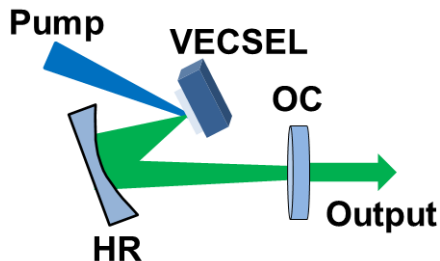

Figure 2. Schematic of the 3-mirror cavity VECSEL. HR: high reflectors. OC: output coupler.

coupling and 10 °C water coolant temperature, the VECSEL emitted up to 17.5 W for 88 W input power with 27% slope efficiency. With the insertion of a 2 mm-thick quartz birefringent filter the laser emission was tunable from 1141.7-1202.7 nm (i.e. 61 nm tuning range) for an input pump power of 43 W. The power transfer and the tuning curve are depicted in Figure 3. These results are comparable to the ones reported in [5].
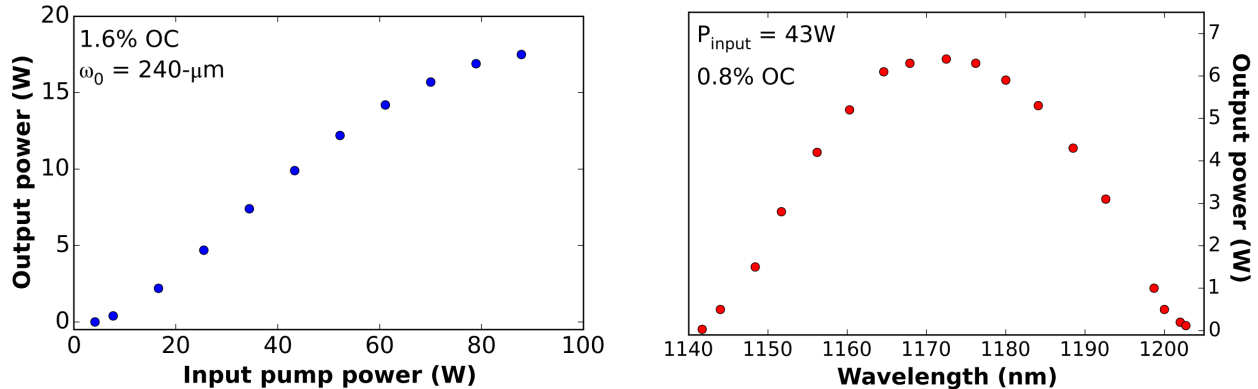

Figure 3. (Left) Power transfer characteristic of the 1180-nm VECSEL with 1.6% output coupling; (Right) Wavelength tuning at 43-W input pump power using a 2-mm quartz birefringent filter and a 0.8% output coupler.

3. INTRACAVITY RAMAN CONVERSION

3.1 Experimental setup

The experimental configuration of the VECSEL-pumped Raman laser is illustrated in Figure 4. The 808 nm pump laser was focused up to 200 µm radius onto the VECSEL gain chip. The Raman resonator was intracavity-pumped within an all-high reflector (R>99.98% at 1150-1400 nm) four-mirror VECSEL cavity. The Raman resonator was separated from the fundamental by a dichroic mirror with high reflection (R>99.9%) at >1290 nm and high transmission (T>99%) at <1200 nm, placed inside the cavity with a small tilt of 5°. The coupled cavity for the Raman field was completed by a plane output coupler (OC) mirror with transmission of ∼2.2% from 1300 to 1350 nm. A 4 mm-thick quartz birefringent filter was inserted at Brewster's angle within the VECSEL cavity, but outside the Raman resonator, to provide spectral narrowing and tuning of the VECSEL, and to pin the fundamental polarization. Both the resonators were aligned to produce a calculated 41 µm TEM$_{00}$ waist radius at the centre of 30 mm-long KGd(WO$_4$)$_2$ (KGW) Raman crystal. The KGW crystal was cut for beam propagation along the N$_p$ axis and both end faces were antireflection coated for 950-1400 nm (R<0.5%). The crystal was oriented for Raman excitation along the N$_m$ axis to access the 901 cm^{-1} Stokes shift [17].
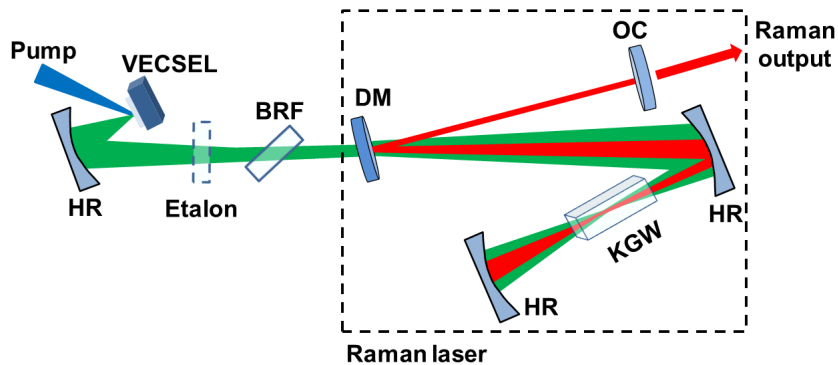

Figure 4. Schematic of the VECSEL-pumped Raman laser for >1300 nm. HR: high reflectors. BRF: birefringent filter. DM: dichroic mirror. OC: output coupler. The etalon plate was only utilized for single-frequency operation experiments.

3.1.1 Results

Figure 5 (Left) shows the power transfers characteristics of the VECSEL-pumped KGW Raman laser with 2.2% output coupling. The Raman laser emitted up to 2.5 W at 1315 nm for an input pump power of 57 W ($>4\%$ diode-to-Stokes conversion efficiency). For higher pump powers, thermal rollover in the VECSEL led to lower output power of the Stokes-shifted field. The Raman laser threshold was achieved for an input pump power of 12.1 W, when the VECSEL intracavity power was around 100 W. Above the Raman threshold, the Stokes-shifted output power increased with pump power with a slope efficiency of 5.7%. Raman conversion led to substantial spectral broadening of the VECSEL emission, and consequently of the Raman laser, as shown in Figure 5 (Right). This effect has been reported in several intracavity Raman laser systems [12, 14, 18] where the fundamental gain bandwidth is larger than the Raman gain linewidth [18]. Due to their broad gain bandwidth, VECSELs are prone to spectral broadening during Raman conversion; however this can be prevented, or at least limited, by the presence of intracavity wavelength filters. It is important to notice that spectral broadening is actually detrimental for the performance of the Raman laser [18,19]. In an ideal intracavity Raman laser the fundamental intracavity power should clamp at its value at the Raman threshold [20], but here the VECSEL intracavity power keeps increasing above Raman threshold. The fundamental intracavity power nearly clamps only for input pump powers greater than 30 W, when the VECSEL and the Raman spectra have similar emission linewidths. At the maximum output power the emission linewidths of the VECSEL and the Raman were measured to be ∼0.7 nm (∼5 cm^{-1}) and ∼0.9 nm (∼5 cm^{-1}) FWHM, respectively. It is interesting to notice that both spectra show several peaks, but apparently they are not related to an etalon effect as in [14]. As a matter of fact, the observed peak separation of ∼0.55 nm does not correspond to an etalon effect due to the heatspreader or the dichroic mirror, although we do not rule out they may contribute somehow. We note, however, that spectral broadening with multi-peak emission has also been reported in [18]. The beam quality factors of the Raman laser and the VECSEL at maximum output power were measured to be ∼2.7 and >3, respectively. Beam quality degradation is commonly observed in intracavity Raman lasers and contributes to the suppression of the expected clamping of the fundamental intracavity power [14,19].

Wavelength tuning of the VECSEL, and consequently of the Raman laser, was achieved by rotating the birefringent filter. The VECSEL emission was tuned from 1160 to 1196 nm, limited by the free spectral range of the 4 mm-thick birefringent filter. Figure 6 shows that the Raman laser was tunable from 1295 to 1340 nm with ∼2.2% output coupling. The whole tuning range of the VECSEL was Stokes shifted. During Raman conversion, the VECSEL and the Raman spectra were both broadened (∼5 cm^{-1} FWHM) over the full tuning range.

3.1.2 Single-frequency operation

To reduce the spectral broadening of the fundamental emission during Raman conversion, we inserted an uncoated 100 μm-thick Suprasil etalon plate in the VECSEL cavity, outside the Raman resonator. The free spectral range of
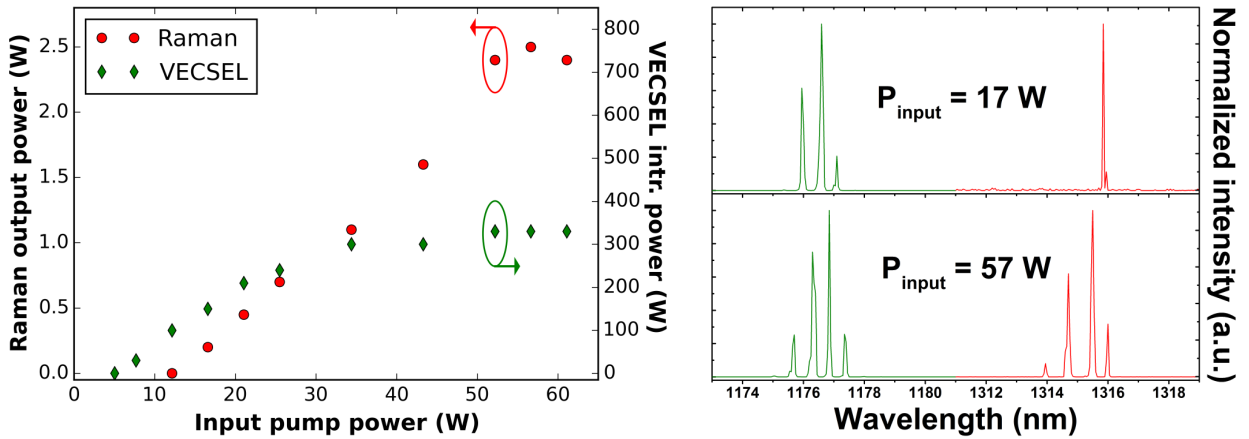

Figure 5. (Left) Power transfer characteristics of the Raman laser (red circles) and the VECSEL (green diamonds) for 2.2% output coupling at 1315 nm; (Right) VECSEL (green line) and Raman laser (red line) spectral emissions near Raman threshold and at the maximum output power.
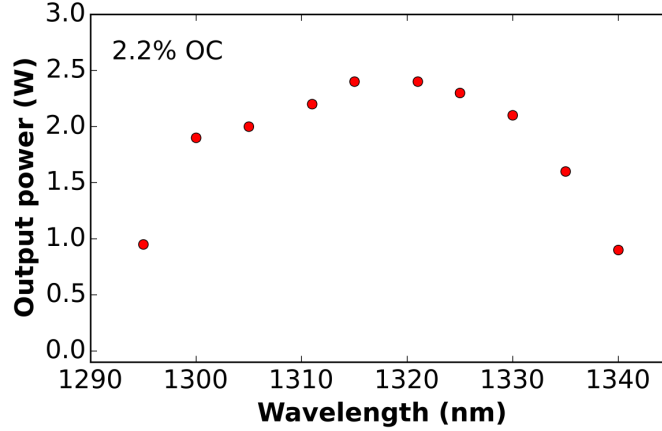
4

Figure 6. Raman laser tuning curve for an input pump power of 57 W with 2.2% output coupling.

this etalon is calculated to be ∼4.8 nm, which proved to be enough to suppress fundamental spectral broadening. Figure 7 shows the power transfers and the spectral characteristics of the VECSEL and the Raman laser using this configuration. Both lasers emitted a single narrow peak, with a measured linewidth of <0.2 nm (<0.15 cm⁻¹) FWHM. The slope efficiency of the Raman emission was calculated to be 6.7%. Raman threshold was achieved for an intracavity fundamental power of ∼100 W (as in the other system), but above Raman threshold it only increased slightly, up to ∼115 W. This suggests that with the insertion of the etalon plate, the effective Raman gain ($g_e \sim A_e/P_f$, where A_e and P_f are the effective area for Raman conversion and the fundamental intracavity power, respectively - see Refs. [15, 19]) above the Raman threshold is higher than in the previous configuration (up to 3 times if A_e is unchanged). This is consistent with the results reported in [18]. However, despite the larger effective Raman gain, the maximum output power of the Raman laser was limited to 1.8 W. We note that with the insertion of the etalon plate thermal rollover occurs at lower pump power (∼45-50 W) than without it (>57 W), hinting that the VECSEL losses have increased. Besides, despite the fact that the fundamental intracavity power clamped, here the slope efficiency of the Raman laser is nearly unchanged (∼6.7%, while in the other setup is 5.7%); a possible explanation is that the increased losses in the VECSEL led to a reduction in its internal efficiency [21], thus affecting the slope efficiency of the Raman laser [14, 19].
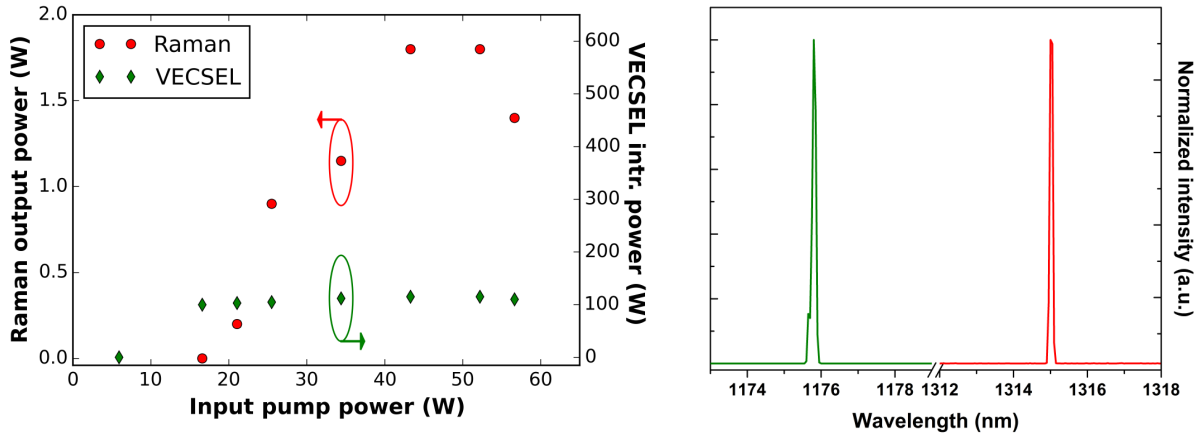

Figure 7. (Left) Power transfer characteristics of the Raman laser (red circles) and the VECSEL (green diamonds) for 2.2% output coupling at 1315 nm; (Right) VECSEL (green line) and Raman laser (red line) spectral emissions at the maximum output power.

4. CONCLUSION

We report intracavity Raman conversion of an 1180 nm InGaAs VECSEL. Output power up to 2.5 W at 1315 nm, with diode-to-Stokes conversion efficiency >4%, $M^2 \sim 2.7$, and relatively broad emission (~ 5 cm^{-1} FWHM) was achieved. The Raman laser was tunable from 1295 to 1340 nm, limited by the free spectral range of the birefringent filter. With the insertion of an additional etalon plate, the Raman laser emitted up to 1.8 W, with narrow emission linewidth (<1.5 cm^{-1} FWHM). Intracavity Raman conversion extends the spectral coverage of InGaAs VECSELs beyond 1300 nm. Work is ongoing to improve the performance of the reported system.

ACKNOWLEDGMENTS

REFERENCES

[1] Okhotnikov (editor), O., [*Semiconductor Disk Lasers: Physics and Technology*], Wiley-VCH (2010).

[2] Calvez, S., Hastie, J. E., Guina, M., Okhotnikov, O. G., and Dawson, M. D., "Semiconductor disk lasers for the generation of visible and ultraviolet radiation," *Laser & Photonics Reviews* **3**, 407–434 (Sept. 2009).

[3] Hein, A., Demaria, F., Kern, A., Menzel, S., Rinaldi, F., Rosch, R., and Unger, P., "Efficient 460-nm second-harmonic generation with optically pumped semiconductor disk lasers," *IEEE Photonics Technology Letters* **23**, 179–181 (Feb. 2011).

[4] Heinen, B., Wang, T.-L., Sparenberg, M., Weber, A., Kunert, B., Hader, J., Koch, S., Moloney, J., Koch, M., and Stolz, W., "106 W continuous-wave output power from vertical-external-cavity surface-emitting laser," *Electronics Letters* **48**, 516–517 (Apr. 2012).

[5] Ranta, S., Tavast, M., Leinonen, T., Van Lieu, N., Fetzer, G., and Guina, M., "1180 nm VECSEL with output power beyond 20 W," *Electronics Letters* **49**, 59–60 (Jan. 2013).

[6] Stothard, D. J. M., Hopkins, J.-M., Burns, D., and Dunn, M. H., "Stable, continuous-wave, intracavity, optical parametric oscillator pumped by a semiconductor disk laser (VECSEL)," *Optics Express* **17**, 10648–10658 (June 2009).

[7] Hopkins, J.-M., Smith, S., Jeon, C., Sun, H., Burns, D., Calvez, S., Dawson, M., Jouhti, T., and Pessa, M., "0.6 W CW GaInNAs vertical external-cavity surface emitting laser operating at 1.32 μm," *Electronics Letters* **40**, 30–31 (Jan. 2004).

[8] Lyytikäinen, J., Rautiainen, J., Toikkanen, L., Sirbu, A., Mereuta, A., Caliman, A., Kapon, E., and Okhotnikov, O. G., "1.3-μm optically-pumped semiconductor disk laser by wafer fusion," *Optics Express* **17**, 9047–9052 (May 2009).

[9] Korpijärvi, V.-M., Leinonen, T., Puustinen, J., Härkönen, A., and Guina, M. D., "11 W single gain-chip dilute nitride disk laser emitting around 1180 nm," *Optics Express* **18**, 25633–25641 (Dec. 2010).

[10] Keller, S., Sirbu, A., Iakovlev, V., Caliman, A., Mereuta, A., and Kapon, E., "8.5 W VECSEL output at 1270 nm with conversion efficiency of 59 %," *Optics Express* **23**, 17437–17442 (June 2015).

[11] Pask, H. M., "Continuous-wave, all-solid-state, intracavity Raman laser," *Optics Letters* **30**(18), 2454–2456 (2005).

[12] Fan, L., Fan, Y., Li, Y., Zhang, H., Wang, Q., Wang, J., and Wang, H., "High-efficiency continuous-wave Raman conversion with a BaWO4 Raman crystal," *Optics Letters* **34**, 1687–1689 (June 2009).

[13] Parrotta, D. C., Lubeigt, W., Kemp, A. J., Burns, D., Dawson, M. D., and Hastie, J. E., "Continuous-wave Raman laser pumped within a semiconductor disk laser cavity," *Optics Letters* **36**, 1083–1085 (Apr. 2011).

[14] Parrotta, D. C., Kemp, A. J., Dawson, M. D., and Hastie, J. E., "Multiwatt, continuous-wave, tunable diamond Raman laser with intracavity frequency-doubling to the visible region," *IEEE Journal of Selected Topics in Quantum Electronics* **19**, 1400108–1400108 (July 2013).

[15] Schlosser, P. J., Parrotta, D. C., Savitski, V. G., Kemp, A. J., and Hastie, J. E., "Intracavity Raman conversion of a red semiconductor disk laser using diamond," *Optics Express* **23**, 8454–8461 (Apr. 2015).

[16] Kantola, E., Leinonen, T., Ranta, S., Tavast, M., and Guina, M., "High-efficiency 20 W yellow VECSEL," *Optics Express* **22**, 6372–6380 (March 2014).

[17] Mochalov, I. V., "Laser and nonlinear properties of the potassium gadolinium tungstate laser crystal $KGd(WO_4)_2$:Nd^{3+}-(KGW:Nd)," *Optical Engineering* **36**, 1660–1669 (June 1997).

[18] Bonner, G. M., Lin, J., Kemp, A. J., Wang, J., Zhang, H., Spence, D. J., and Pask, H. M., "Spectral broadening in continuous-wave intracavity Raman lasers," *Optics Express* **22**, 7492–7502 (Apr. 2014).

[19] Spence, D. J., "Spatial and spectral effects in continuous-wave intracavity Raman lasers," *IEEE Journal of Selected Topics in Quantum Electronics* **21**, 134–141 (Jan. 2015).

[20] Spence, D. J., Dekker, P., and Pask, H. M., "Modeling of continuous wave intracavity Raman lasers," *IEEE Journal of Selected Topics in Quantum Electronics* **13**, 756 –763 (May-June 2007).

[21] Maclean, A. J., Birch, R. B., Roth, P. W., Kemp, A. J., and Burns, D., "Limits on efficiency and power scaling in semiconductor disk lasers with diamond heatspreaders," *J. Opt. Soc. Am. B* **26**, 2228–2236 (Dec. 2009).